

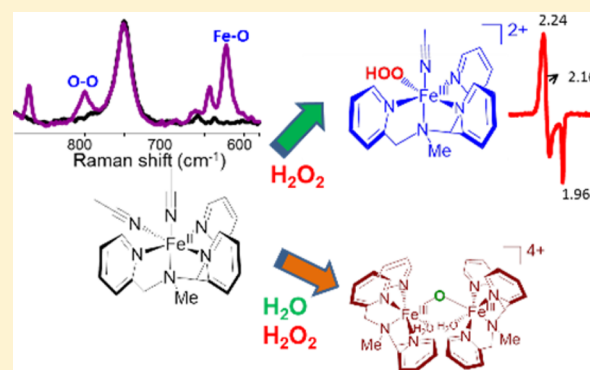
# Conflicting Role of Water in the Activation of H<sub>2</sub>O<sub>2</sub> and the Formation and Reactivity of Non-Heme Fe<sup>III</sup>–OOH and Fe<sup>III</sup>–O–Fe<sup>III</sup> Complexes at Room Temperature

Sandeep K. Padamati, Apparao Draksharapu, Duenpen Unjaroen, and Wesley R. Browne\*

Molecular Inorganic Chemistry, Stratingh Institute for Chemistry, Faculty of Mathematics and Natural Sciences, University of Groningen, Nijenborgh 4, 9747AG, Groningen, The Netherlands

## Supporting Information

**ABSTRACT:** The formation of an Fe<sup>III</sup>–OOH species by reaction of complex **1** [(MeN3Py)Fe<sup>II</sup>(CH<sub>3</sub>CN)<sub>2</sub>]<sup>2+</sup> with H<sub>2</sub>O<sub>2</sub> at room temperature is reported and is studied by a combination of UV/vis absorption, EPR, and resonance Raman spectroscopies. The formation of the Fe<sup>III</sup>–OOH species, and its subsequent conversion to relatively inert Fe<sup>III</sup>–O–Fe<sup>III</sup> species, is shown to be highly dependent on the concentration of water, with excess water favoring the formation of the latter species, which is studied by UV/vis absorption spectroelectrochemistry also. The presence of acetic acid increases the rate and extent of oxidation of **1** to its iron(III) state and inhibits the wasteful decomposition of H<sub>2</sub>O<sub>2</sub> but does not affect significantly the spectroscopic properties of the Fe<sup>III</sup>–OOH species formed.



## INTRODUCTION

Synthetic nonheme iron complexes that activate H<sub>2</sub>O<sub>2</sub> are of increasing interest as models for nonheme mononuclear iron-dependent oxygenases<sup>1</sup> and in the catalytic oxidation of C–H bonds.<sup>2–4</sup> The development of synthetic catalytic systems presents many opportunities in both achieving selective and efficient oxidations under ambient conditions and allowing access to reactive species that provide insight into the mechanism by which nonheme iron-dependent enzymes achieve a wide range of oxidative transformations, e.g., the oxidation of arenes by Rieske oxygenases.<sup>5</sup> The oxidation of alkenes to epoxides and 1,2-diols is of synthetic as well as biomimetic interest,<sup>6</sup> and in recent years several nonheme complexes have been shown to be particularly useful in this regard.<sup>7</sup> In particular, iron complexes that present two solvent-accessible sites, as is found for example in naphthalene dioxygenase, which ligates Fe(II) with two histidines and a bidentate aspartic acid,<sup>8</sup> are of particular interest in that they can use H<sub>2</sub>O<sub>2</sub> as terminal oxidant<sup>9,10</sup> and because of the “water-assisted” mechanism by which putative iron(V)=O species are proposed to be formed from (HO)Fe<sup>III</sup>–OOH<sup>11</sup> and (AcO)–Fe<sup>III</sup>–OOH<sup>12</sup> intermediates. Notable examples include complexes bearing tetradentate (N<sub>4</sub>) ligands such as [(TPA)–Fe<sup>II</sup>(CH<sub>3</sub>CN)<sub>2</sub>]<sup>2+</sup> and [(TMC)Fe<sup>II</sup>(CH<sub>3</sub>CN)<sub>2</sub>]<sup>2+</sup> (where TPA is tris(2-pyridylmethyl)amine and TMC is 1,4,8,11-tetraazaazacyclotetradecane), reported by Que and co-workers,<sup>13</sup> and [(MeN3Py)Fe<sup>II</sup>(CH<sub>3</sub>CN)<sub>2</sub>](ClO<sub>4</sub>)<sub>2</sub> (**1**) (Figure 1, where MeN3Py is 1,1-di(pyridin-2-yl)-N-methyl-N-(pyridin-2-ylmethyl)methanamine) reported by Feringa and co-workers, which were shown to be active in alkene dihydroxylation, as

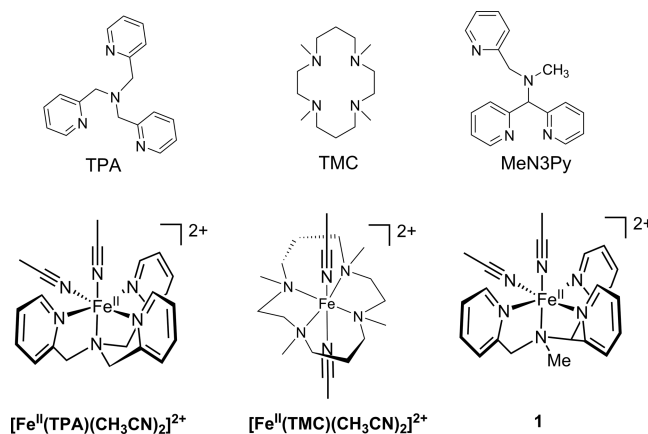
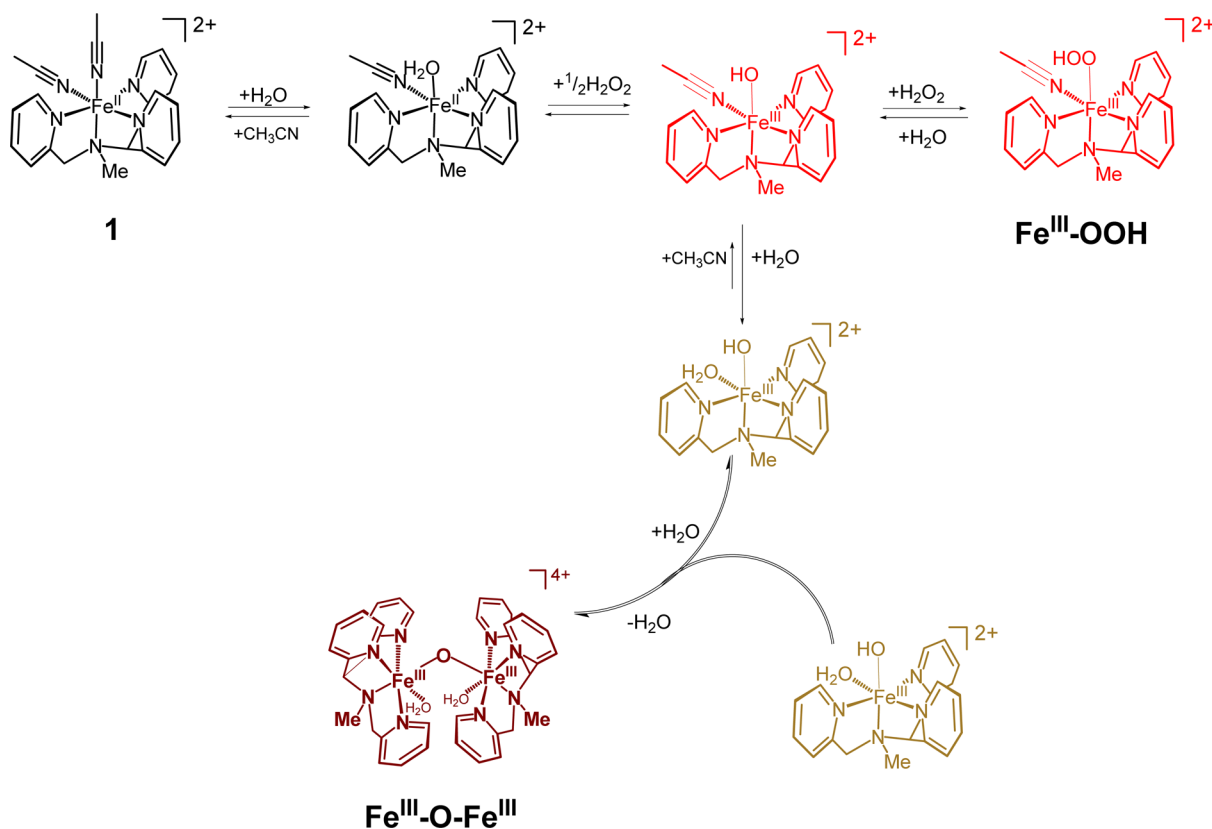


**Figure 1.** Ligands and corresponding Fe(II) complexes discussed in the text.

well as epoxidation.<sup>14</sup> With notable exceptions, the involvement of Fe<sup>III</sup>–OOH intermediates has only been inferred in the case of iron(II) complexes of N<sub>4</sub> donor ligands,<sup>14</sup> in contrast to their related N<sub>5</sub> donor ligands and bleomycin,<sup>9,15</sup> for which such intermediates have been characterized thoroughly. The observation of N<sub>4</sub>–Fe<sup>III</sup>–OOH species under ambient conditions is rarer still.<sup>16</sup> Nevertheless, it is generally considered that, even if formed, Fe<sup>III</sup>–OOH species do not engage directly in oxygenation of substrates and C–H abstraction, but are

Received: December 27, 2015

**Scheme 1. Aquation of Complex 1 and Subsequent Oxidation by H<sub>2</sub>O<sub>2</sub> Yields Fe<sup>III</sup>-OH, Which Undergoes Ligand Exchange to Form an Fe<sup>III</sup>-OOH Species in Competition with Thermodynamically Stable Fe<sup>III</sup>-O-Fe<sup>III</sup> Complexes**



instead precursors to reactive high-valent Fe<sup>IV</sup>=O and Fe<sup>V</sup>=O species.<sup>17</sup> Hence, identifying and determining the intrinsic reactivity of Fe<sup>III</sup>-OOH species is important from a fundamental perspective.

In this contribution, we show that an Fe<sup>III</sup>-OOH species is generated upon reaction of **1** with H<sub>2</sub>O<sub>2</sub>. Under appropriate conditions, we found that this species is sufficiently stable to be studied at room temperature by a combination of UV/vis absorption, electron paramagnetic resonance (EPR), and Raman spectroscopies. Furthermore, we demonstrate that the formation of this Fe<sup>III</sup>-OOH species, and its subsequent conversion to a relatively inert Fe<sup>III</sup>-O-Fe<sup>III</sup> species, is highly dependent on the concentration of water. In particular, the reaction of the iron(II) complex **1** with H<sub>2</sub>O<sub>2</sub> in acetonitrile requires that a thermodynamically unfavorable ligand exchange with water takes place initially. Hence, the concentration of water determines the rate and extent of oxidation of **1** to an Fe<sup>III</sup>-OH species and thereby the rate of the formation of the Fe<sup>III</sup>-OOH species. Importantly, however, the water content also affects the rate of formation of inert Fe<sup>III</sup>-O-Fe<sup>III</sup> complexes from Fe<sup>III</sup>-OH species. Hence accelerating the rate of initial oxidation of **1** by increasing the concentration of water must be balanced with the increase in the rate of the subsequent formation of Fe<sup>III</sup>-O-Fe<sup>III</sup> complexes, which act as thermodynamic sinks.<sup>11a,18</sup> Furthermore, we show that the presence of acetic acid, which has been shown in many cases to enhance the efficiency of N4-donor ligand based catalysts,<sup>19</sup> increases the rate and extent of oxidation of **1** to its iron(III) state, in large part by inhibiting the wasteful decomposition of H<sub>2</sub>O<sub>2</sub>. Importantly, however, acetic acid does not affect significantly the spectroscopic properties of the Fe<sup>III</sup>-OOH

species formed. Finally we show that the formation and loss of the Fe<sup>III</sup>-OOH species are not significantly affected by the presence of alkenes, indicating that it is a resting state in the catalytic cycle. A summary of the processes studied is shown in Scheme 1.

## RESULTS

The synthesis and X-ray structural characterization of [(Me<sub>3</sub>N<sub>3</sub>Py)Fe<sup>II</sup>(CH<sub>3</sub>CN)<sub>2</sub>](ClO<sub>4</sub>)<sub>2</sub> (**1**) was reported earlier.<sup>14</sup> The Raman spectra of **1** in the solid state and in acetonitrile (see the Supporting Information, Figure S1) indicate that the molecular structure of **1** in the solid state is retained in solution. The <sup>1</sup>H NMR spectrum of **1** in CD<sub>3</sub>CN (Figure S2) shows signals in the range 0–15 ppm, as expected for a low-spin iron(II) complex, with increased broadening and shift to lower fields when compared with the spectra of related low-spin N4 iron(II) complexes such as [(TPA)Fe<sup>II</sup>(CH<sub>3</sub>CN)<sub>2</sub>](ClO<sub>4</sub>)<sub>2</sub>.<sup>20</sup> The broadening is ascribed to slow exchange, on the NMR time scale, between the CH<sub>3</sub>CN ligands with adventitious H<sub>2</sub>O to form the high-spin complex [(Me<sub>3</sub>N<sub>3</sub>Py)Fe<sup>II</sup>(CH<sub>3</sub>CN)-(H<sub>2</sub>O)]<sup>2+</sup>. The rate of exchange was increased by addition of D<sub>2</sub>O (1 M), which resulted in further broadening of the signals and shifting to lower field (20–120 ppm, Figure S2). These data indicate that the reversible exchange of acetonitrile ligands for D<sub>2</sub>O is rapid on the <sup>1</sup>H NMR time scale; however, the equilibrium lies toward the acetonitrile-bound complex, as confirmed by UV/vis absorption spectroscopy and cyclic voltammetry (vide infra).

**1** shows two electronic absorption bands in the visible region (359 and 429 nm), which are assigned to metal-to-ligand charge transfer (<sup>1</sup>MLCT) transitions (vide infra), and a pyridyl-

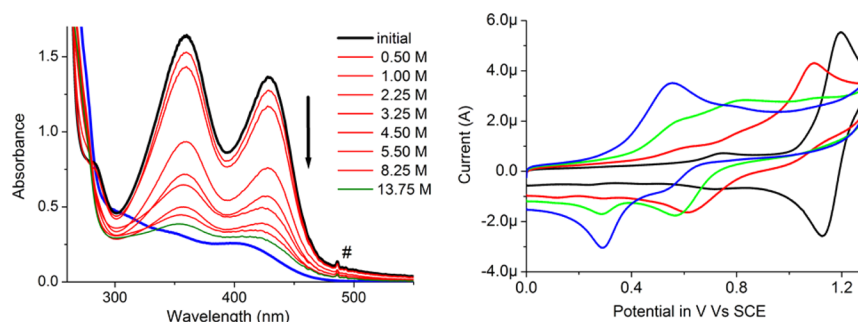


**Figure 2.** (Left) UV/vis absorption spectra of **1** (0.25 mM) in water (blue line), in acetonitrile (black line), and in acetonitrile with increasing amounts of water (0.5 to 8.25 M (red lines) and 13.75 M (green line)). Spectra are corrected for dilution. # instrumental artifact. (Right) Cyclic voltammetry of **1** (0.25 mM) in acetonitrile (0.1 M TBAPF<sub>6</sub>) with H<sub>2</sub>O: 0.00 M (black), 1.25 M (red), 2.5 M (green), and 3.75 M (blue).

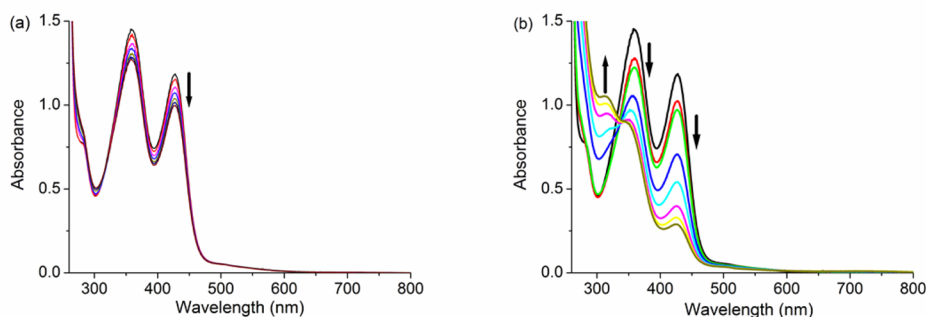


**Figure 3.** UV/vis absorption spectra of **1** (0.25 mM, black line) in acetonitrile (a) (4, 25, 50, 100, 150, and 200 s) after addition of 1 equiv of H<sub>2</sub>O<sub>2</sub> and (b) after addition of H<sub>2</sub>O (1.25 M, red line) followed by 1 equiv of H<sub>2</sub>O<sub>2</sub> (2, 25, 50, 100, 150, and 200 s).

centered  $\pi \rightarrow \pi^*$  transition between 200 and 300 nm (by comparison with the absorption spectrum of the unbound ligand).<sup>21</sup>

A blue shift and broadening of the visible absorption bands as well as a substantial decrease in molar absorptivity (ca. 70%) are observed in water compared to acetonitrile (Figure 2). There is a substantial decrease in the visible <sup>1</sup>MLCT absorption bands only upon addition of >1 M H<sub>2</sub>O (Figure 2). Addition of H<sub>2</sub>O (13.75 M) results in a blue shift in the pyridyl-centered  $\pi \rightarrow \pi^*$  transitions and a broadening and decrease in the visible absorption bands, resulting in a spectrum (Figure 2, green line) similar to that observed in water alone (Figure 2, blue line). The two spectra are not exactly the same, but it should be noted that the absorption spectra of complexes such as **1** show a pronounced pH dependence,<sup>21</sup> and hence it can be concluded that with >8 M H<sub>2</sub>O both acetonitrile ligands are exchanged with H<sub>2</sub>O. Indeed, addition of acetonitrile (2–25 vol %) to an aqueous solution of **1** did not affect the UV/vis absorption spectrum obtained in water (Figure S3).<sup>14,21</sup> The <sup>1</sup>H NMR spectrum of **1** in acetonitrile is affected to a greater extent by the addition of water than the UV/vis absorption spectrum, indicating that the exchange of acetonitrile and aqua ligands is rapid. The effect of water on both the UV/vis absorption and <sup>1</sup>H NMR spectra are consistent with exchange of the acetonitrile ligands with water to form high-spin Fe(II) complexes (i.e., where one and then both of the acetonitrile ligands are exchanged).<sup>22</sup> The ligand field strength of the aqua ligands is much less than that of acetonitrile, and hence the concomitant switch to a high-spin (presumably quintet) state results in a decrease in molar absorptivity of the MLCT bands (<sup>1</sup>MLCT vs <sup>5</sup>MLCT).

**1** undergoes reversible oxidation (Fe<sup>III</sup>/Fe<sup>II</sup>(CH<sub>3</sub>CN)<sub>2</sub> redox couple) at 1.14 V vs SCE. Addition of water (1.25 M) renders the oxidation chemically irreversible (due to rapid ligand exchange (CH<sub>3</sub>CN/H<sub>2</sub>O) in the Fe<sup>III</sup> state) and shifts the peak potential ( $E_{p,a}$ ) to 1.0 V vs SCE (due to electrostatic stabilization).<sup>21,23</sup> On the return cycle toward negative potentials a new reversible redox wave is observed at 0.65 V vs SCE, assigned, tentatively, to the Fe<sup>III</sup>/Fe<sup>II</sup>(OH<sub>2</sub>)(CH<sub>3</sub>CN) redox couple, in addition to reduction waves at 0.35 and 0.15 V vs SCE (Figure 2, right) assigned to fully aquated species and a  $\mu$ -oxido-bridged dinuclear complex (vide infra). Further addition of water (up to 3.75 M) resulted in a complete loss of the redox wave at 1.0 V and the appearance of a new redox wave at  $E_{p,a}$  0.4 V due to the formation of the aquated complexes [LFe<sup>II</sup>(CH<sub>3</sub>CN)(H<sub>2</sub>O)]<sup>2+</sup> and eventually [LFe<sup>II</sup>(H<sub>2</sub>O)<sub>2</sub>]<sup>2+</sup>, and on the reverse scan only the reduction at 0.3 V is observed, indicating rapid ligand exchange and deprotonation of the aqua ligands in the more acidic iron(III) state, with respect to the electrochemical time scale (Figure 2, right).

In water (pH 6.5), **1** shows a reversible redox wave at ca. 0.40 V vs SCE ascribed to an Fe<sup>III</sup>/Fe<sup>II</sup>(OH<sub>2</sub>) redox couple and a reduction wave at 0.28 V vs SCE (Figure S4).<sup>21</sup> Addition of acetonitrile (to 1.25 M) results in only a minor decrease (15%) in peak current of the Fe<sup>III</sup>/Fe<sup>II</sup>(OH<sub>2</sub>) redox wave. Consistent with the UV/vis absorption spectral data (Figure S3), the redox wave at ca. 1.0 V did not appear upon addition of acetonitrile.

Resonance Raman spectra of **1** in acetonitrile were recorded at  $\lambda_{exc}$  355 and 457 nm (i.e., in resonance with the absorption bands at 359 and 429 nm, Figures S5 and S6, respectively). The bands at 1613, 1571, 1555, 1296, 1282, 1157, and 656 cm<sup>-1</sup> are assigned to pyridyl-based vibrational modes in comparison with

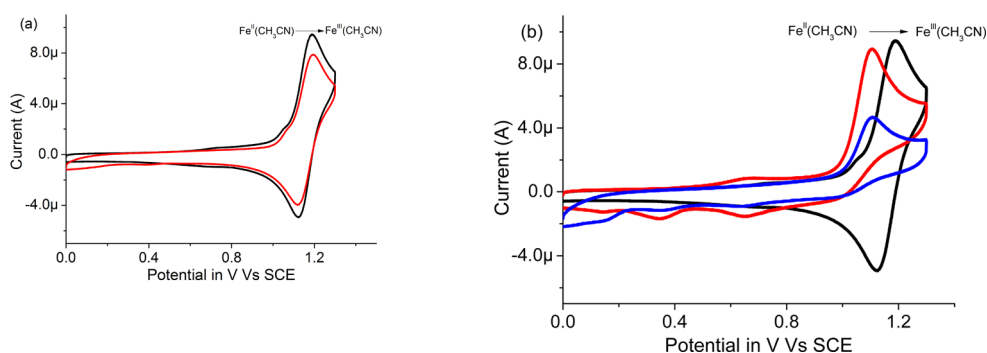


**Figure 4.** Cyclic voltammetry of **1** in acetonitrile (0.5 mM, 0.1 M TBAPF<sub>6</sub>) (a) before (black) and after addition of 1 equiv of H<sub>2</sub>O<sub>2</sub> (red) and (b) before (black) and after addition of H<sub>2</sub>O (0.5 M, red) and subsequent addition of 1 equiv of H<sub>2</sub>O<sub>2</sub> (blue). For data for **1** at 0.25 mM see Figure S8.

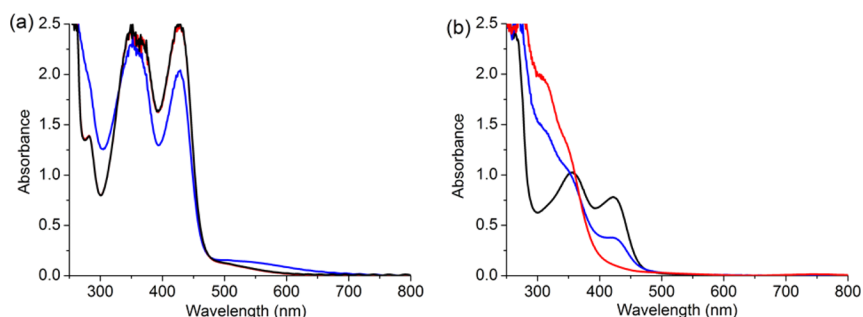


**Figure 5.** UV/vis absorption at 278 K of **1** (0.5 mM) (a) in acetonitrile and (b) in acetonitrile with water (5.5 M, black) before (black) and 2 s (red) and 100 s (blue) after addition of 1 equiv of H<sub>2</sub>O<sub>2</sub>.

the Raman spectrum of [Fe(bpy)<sub>3</sub>]<sup>2+</sup> (1608, 1565, 1492, 1322, 1278, 1175, 1026 cm<sup>-1</sup>)<sup>24</sup> and are consistent with assignment of both absorption bands as <sup>1</sup>MLCT bands. The modes at 1297, 1223, and 1201 cm<sup>-1</sup> are assigned to the modes of the alkyl amine backbone of the ligands by comparison with [(N4Py)Fe<sup>II</sup>(CH<sub>3</sub>CN)]<sup>2+</sup>.<sup>21</sup> Addition of water (1.25 M) results in a decrease in the intensity of the Raman bands of the complex (Figures S5 and S6), which is consistent with the decrease in absorption observed at both wavelengths (Figure 2).

**Reaction of **1** with H<sub>2</sub>O<sub>2</sub> in Acetonitrile.** Addition of 1 equiv of H<sub>2</sub>O<sub>2</sub> to **1** in acetonitrile resulted in only a 10% decrease in absorbance at 429 and 359 nm (over 200 s) and a concomitant increase in absorbance at 310 nm. No change in absorbance was observed at longer wavelengths (Figure 3a). In contrast, addition of 1 equiv of H<sub>2</sub>O<sub>2</sub> to **1** in acetonitrile with water (1.25 M) results in a faster (ca. 10-fold) and greater extent of decrease in absorbance (by ca. 80%) in the visible region with a concomitant increase in absorbance at 310 nm with maintenance of an isosbestic point at 340 nm (Figure 3b).

Addition of 1 equiv of H<sub>2</sub>O<sub>2</sub> had relatively little effect on the Fe<sup>III</sup>/Fe<sup>II</sup>(CH<sub>3</sub>CN) redox couple (Figure 4a), with only a minor decrease in *I*<sub>p,a</sub> (corresponding to the decrease observed in visible absorption). Addition of 10 equiv of H<sub>2</sub>O<sub>2</sub> results in a 50% decrease in *I*<sub>p,a</sub>, however, no new redox waves were observed, and the reversibility of the Fe<sup>III</sup>/Fe<sup>II</sup>(CH<sub>3</sub>CN) redox was maintained (Figure S7). Addition of water (0.5 M) renders the Fe<sup>III</sup>/Fe<sup>II</sup>(CH<sub>3</sub>CN) redox couple of **1** irreversible, although *I*<sub>p,a</sub> remains relatively unchanged, and *E*<sub>p,a</sub> shifts to a slightly less positive potential (vide supra). In addition, on the return cycle, new reduction waves at 0.63, 0.36, and 0.14 V vs SCE are observed, which are consistent with exchange of CH<sub>3</sub>CN for H<sub>2</sub>O being favored in the Fe(III) oxidation state. Subsequent

addition of 1 equiv of H<sub>2</sub>O<sub>2</sub> resulted in a ca. 60% decrease in the *I*<sub>p,a</sub> of the Fe<sup>III</sup>/Fe<sup>II</sup>(CH<sub>3</sub>CN) redox couple (Figure 4b), in agreement with changes observed by UV/vis spectroscopy (Figure 3b). Notably, the additional redox waves at lower potential disappeared upon addition of H<sub>2</sub>O<sub>2</sub> also, replaced by a reduction wave at 0.2 V (vide infra).

At 278 K the addition of 1 equiv of H<sub>2</sub>O<sub>2</sub> does not affect the absorption spectrum of **1**, and prior addition of excess water (1.25 M) results in only a 20% decrease in visible absorbance (Figure S9). At higher concentration (0.5 mM with 1 equiv of H<sub>2</sub>O<sub>2</sub>) a minor decrease in absorbance at 429 nm occurs. However, in contrast to that observed at 293 K, a concomitant increase (followed by a slower decrease) in absorbance at λ<sub>max</sub> 551 nm<sup>25</sup> (to Abs 0.012) is observed at 278 K over 100 s (Figure 5a). In contrast, similar to that at 293 K, with a large excess of water present (5.5 M), addition of 1 equiv of H<sub>2</sub>O<sub>2</sub> at 278 K to **1** (0.5 mM) results in a rapid and complete loss in absorbance at 429 nm, and no increase in absorbance is observed at 551 nm (Figure 5b). The sensitivity of the system to the concentration of water is remarkable and emphasizes the delicate balance between the rates of the various processes that occur upon addition of H<sub>2</sub>O<sub>2</sub> to **1**.

Hence, although addition of several hundred equivalents of water does not result in significant aquation of **1**, the rate of CH<sub>3</sub>CN/H<sub>2</sub>O ligand exchange is sufficiently rapid to allow for oxidation to the iron(III) state by H<sub>2</sub>O<sub>2</sub> to proceed at a relatively fast overall rate. Notably the observation of an absorption (at 278 K) at 551 nm indicates the formation of a reactive intermediate.

**Reaction of **1** with Excess H<sub>2</sub>O<sub>2</sub>.** Addition of 25 equiv of H<sub>2</sub>O<sub>2</sub> to **1** (0.25 mM) in acetonitrile at 293 K results in a more rapid decrease in the visible absorption than observed with 1 equiv of H<sub>2</sub>O<sub>2</sub>. Furthermore, the transient absorption at 551

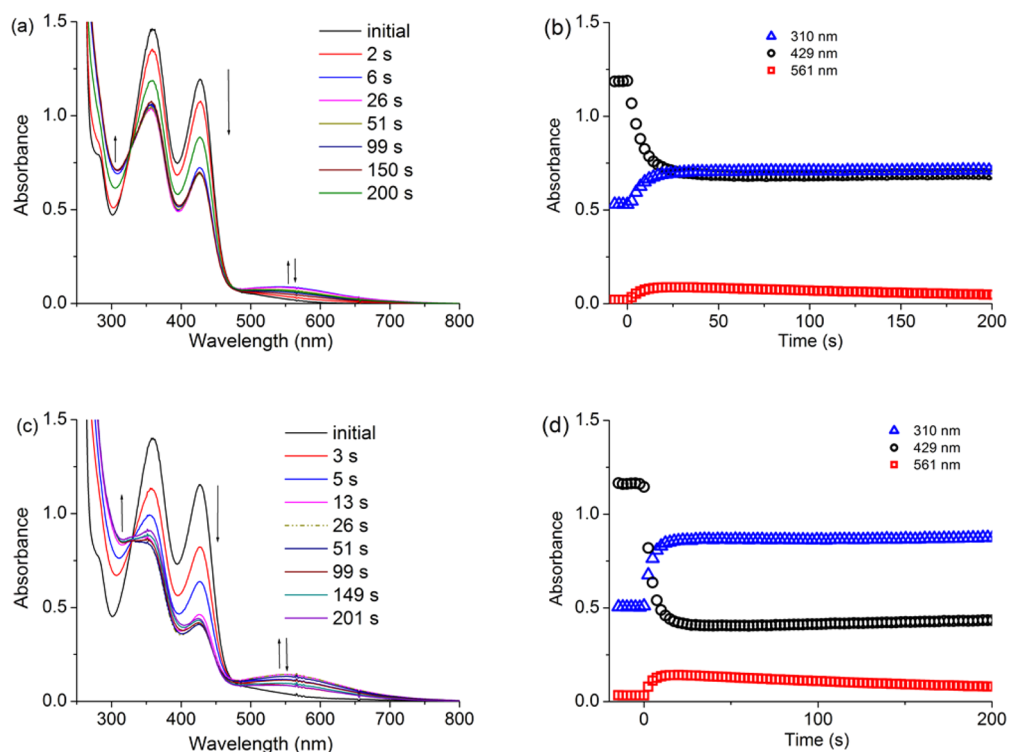


**Figure 6.** UV/vis absorption of **1** (0.25 mM) in acetonitrile at 293 K (a) upon addition of 25 equiv of  $\text{H}_2\text{O}_2$  {(b) corresponding time dependence of absorbance at 310 nm (blue), 429 nm (black), and 561 nm (red)} and (c) upon addition of 100 equiv of  $\text{H}_2\text{O}_2$  {(d) corresponding time dependence of absorbance at 310 nm (blue), 429 nm (black), and 561 nm (red)}.

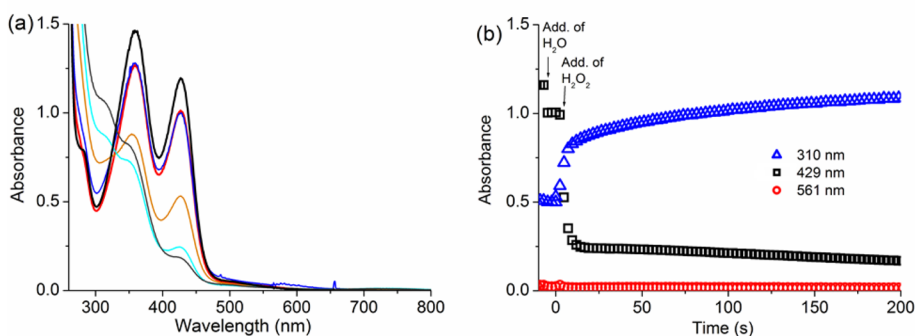


**Figure 7.** UV/vis absorption of **1** (0.25 mM) in acetonitrile (black line) and after addition of water (red line, 1.25 M) at 293 K followed by addition of 25 equiv of  $\text{H}_2\text{O}_2$  (after 2 s (blue), 5 s (orange), 25 s (cyan), and 175 s (gray)) and (b) corresponding time dependence of absorbance at 310 nm (blue), 429 nm (black), and 561 nm (red).

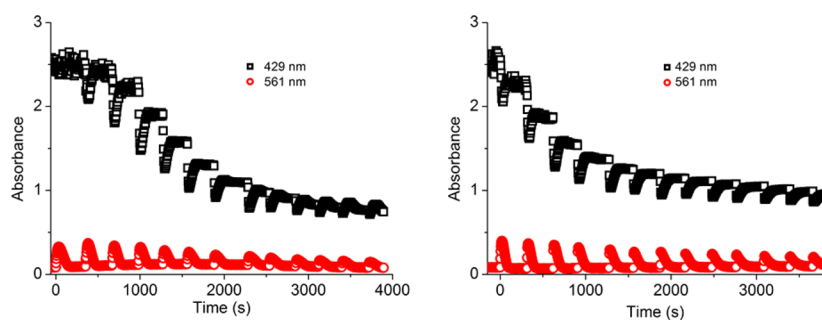


**Figure 8.** Time dependence of the absorbance at 429 and 561 nm following batchwise addition (ca. 7 equiv each) of a total of 100 equiv of  $\text{H}_2\text{O}_2$  to **1** (0.875 mM) in acetonitrile (left) without and (right) with cyclooctene (0.875 M). See Figure S15 for absorption spectra recorded when absorbance at 561 nm was maximum.

nm is observed at 293 K, reaches a maximum (Abs 0.09) within 25 s, and subsequently decreases over 300 s, with a concomitant increase in absorbance at 310 nm (Figure 6a and b; with 100 equiv a maximum of 0.15 is reached within 10 s).<sup>26</sup>

Addition of 100 equiv of H<sub>2</sub>O<sub>2</sub> to **1** in acetonitrile at 278 K resulted in similar changes but with a decrease in the rate of the reaction and an increase in the maximum absorbance (0.14) at 551 nm reached (Figure 6c and d). Again the absorbance at 551 nm decreased (<300 s) concomitant with an increase in absorbance at 310 nm (Figure S10a). Further additions of H<sub>2</sub>O<sub>2</sub> resulted in an increase, although much less than initially, in absorbance at 551 nm (vide infra, Figure 10). In all cases,

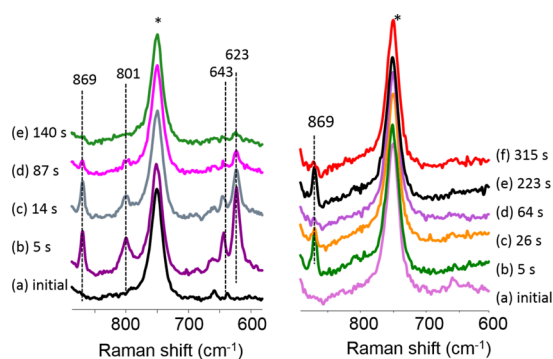


**Figure 9.** Resonance Raman spectra at  $\lambda_{\text{exc}}$  532 nm of (left) (a) **1** in acetonitrile and (b) 5 s, (c) 14 s, (d) 87 s, and (e) 140 s after addition of 100 equiv of H<sub>2</sub>O<sub>2</sub>. (Right) (a) **1** (1 mM) in acetonitrile with 0.55 M water, (b) 5 s, (c) 26 s, and (d) 64 s after addition of 100 equiv of H<sub>2</sub>O<sub>2</sub>, and (e) second addition of 100 equiv of H<sub>2</sub>O<sub>2</sub> at 223 s and (f) 315 s. \*Spectra are normalized to solvent band at 750 cm<sup>-1</sup>.

although complete conversion of **1** to an iron(III) oxidation state was not reached, all of the H<sub>2</sub>O<sub>2</sub> had been consumed by the end of the reaction (vide infra). Changes to the Raman spectra ( $\lambda_{\text{exc}}$  355 nm) are consistent with UV/vis absorption spectroscopic data (Figures S11 and S12).

In contrast addition of 25 or 100 equiv of H<sub>2</sub>O<sub>2</sub> to **1** in acetonitrile with water (1.25 M) present led to the rapid decrease in visible absorbance with a direct concomitant

increase in absorbance at ca. 310 nm and without a significant increase in absorbance at 551 nm (Figure 7 and Figure S11).

**Effect of Alkenes on the Formation and Disappearance of Fe<sup>III</sup>–OOH Species.** The oxidation of alkenes by **1** with H<sub>2</sub>O<sub>2</sub> was reported earlier.<sup>14</sup> The addition of cyclooctene (0.875 M) to **1** (0.875 mM) has no effect on the latter's absorption spectrum, and only a minor effect on the changes to the absorption spectrum of **1** that occur upon addition of H<sub>2</sub>O<sub>2</sub> (Figure S13).<sup>27</sup> Under conditions used in the catalyzed oxidation of alkenes,<sup>14</sup> i.e., periodic addition of H<sub>2</sub>O<sub>2</sub> (100 equiv with respect to **1** in total) over 1 h, the incremental loss of absorbance of **1** and the repeated appearance and subsequent disappearance of the Fe(III)–OOH species are observed (Figure 8, together with the formation of the epoxide and cis-diol products, Figure S15). Notably the loss of absorbance at 429 nm (i.e., of **1**) occurs concomitant with the increase in the absorption band at 551 nm, while the recovery of absorbance at 429 nm occurs concomitant with the decrease in absorption band at 551 nm. This latter increase in absorption at 429 nm is ascribed to formation of Fe<sup>III</sup>–OH and Fe<sup>III</sup>–O–Fe<sup>III</sup> species and not recovery of **1**. Notably, although initially the rate of decrease in the absorbance due to the Fe<sup>III</sup>–OOH species is marginally faster in the presence of cyclooctene, after several additions of H<sub>2</sub>O<sub>2</sub>, the differences in the rates of all processes are marginal, and hence it can be concluded that the Fe<sup>III</sup>–OOH does not react with the alkene itself but instead decomposes to a secondary species, e.g., an Fe<sup>IV</sup>=O species, spontaneously.

**Resonance Raman, EPR, and <sup>1</sup>H NMR Spectroscopy of **1** with H<sub>2</sub>O<sub>2</sub>.** The intermediate species formed, which absorbs at 551 nm, was studied by Raman spectroscopy at  $\lambda_{\text{exc}}$  532 nm.<sup>28</sup> The Raman spectrum recorded upon addition of 100 equiv of H<sub>2</sub>O<sub>2</sub> to **1** in acetonitrile shows bands at 801, 643, and 623 cm<sup>-1</sup> (Figure 9, left).<sup>29</sup> The band at 801 cm<sup>-1</sup> was assigned, tentatively, to an O–O stretch and the band at 623 cm<sup>-1</sup> to the Fe–O stretch of a [(Me-N3Py)Fe<sup>III</sup>(X)(OOH)]<sup>2+</sup> species (where X = solvent), by comparison with related complexes such as [(TPA)Fe<sup>III</sup>(OOH)]<sup>2+</sup> and [(N4Py)-Fe<sup>III</sup>(OOH)]<sup>2+</sup>.<sup>30–32</sup> The band at 643 cm<sup>-1</sup> is assigned tentatively to an Fe–N stretch by analogy with the Raman spectra of related Fe<sup>III</sup>–OCl species.<sup>33</sup> The Raman band at 869 cm<sup>-1</sup> ( $\nu_{\text{s(O-O)}}$  of H<sub>2</sub>O<sub>2</sub>) decreases concomitantly albeit slightly

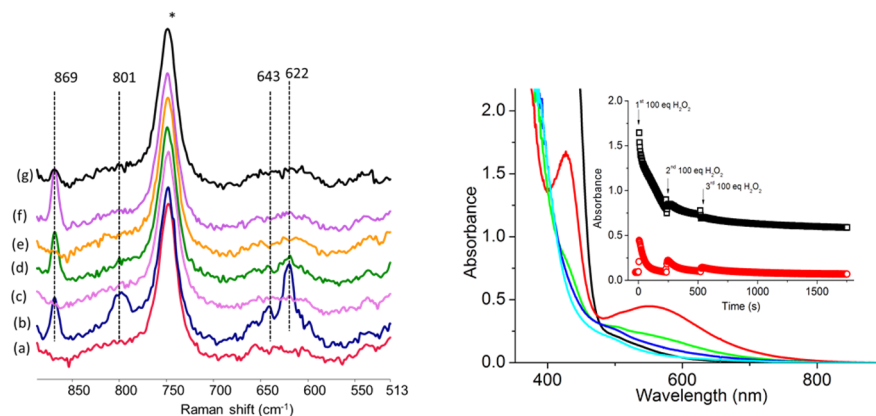


**Figure 10.** (left) Resonance Raman spectra at  $\lambda_{\text{exc}}$  532 nm of (a) **1** in acetonitrile (1 mM), (b) 5 s and (c) 133 s after addition of 100 equiv of H<sub>2</sub>O<sub>2</sub>, (d) second addition of 100 equiv of H<sub>2</sub>O<sub>2</sub> at 167 s and after (e) 508 s, (f) third addition of 100 equiv of H<sub>2</sub>O<sub>2</sub> after 533 s and (g) 972 s. \*Spectra are normalized to solvent band at 750 cm<sup>-1</sup>. (Right) UV/vis absorption spectrum of **1** (1 mM) in acetonitrile (black) upon addition of first (red), second (green), and third (blue) 100 equiv of H<sub>2</sub>O<sub>2</sub> and after 30 min (cyan) with corresponding time dependence of absorbance at 429 nm (black) and 561 nm (red).

faster than the bands at 801 and 623  $\text{cm}^{-1}$ . Addition of further equivalents of  $\text{H}_2\text{O}_2$  do not lead to the reappearance of the bands at 623, 643, and 801  $\text{cm}^{-1}$ , but the consumption of  $\text{H}_2\text{O}_2$  is manifest in the decrease in the Raman band ( $\nu_{\text{s(O-O)}}$  of  $\text{H}_2\text{O}_2$ ) at 869  $\text{cm}^{-1}$  (Figure 10, left). As observed by UV/vis absorbance spectroscopy (vide supra), in the presence of water, the  $\text{Fe}^{\text{III}}\text{-OOH}$  species is not observed; however, the consumption of  $\text{H}_2\text{O}_2$  over several additions is observed by Raman spectroscopy (Figure 9, right).

The X-band EPR spectrum (at 77 K) of **1** in acetonitrile after addition of 1 equiv of  $\text{H}_2\text{O}_2$  in the absence and presence of water showed only a weak signal at  $g = 4.3$ , characteristic for high-spin iron(III) species. In contrast, the EPR spectrum obtained upon flash freezing (at 77 K) of **1** in acetonitrile with 100 equiv of  $\text{H}_2\text{O}_2$  upon reaching a maximum absorbance at 551 nm (Figure 10) shows relatively strong signals at  $g = 2.24$ , 2.16, and 1.96 (Figure 11), assigned<sup>16,34</sup> to a  $[(\text{MeN3Py})\text{-}$

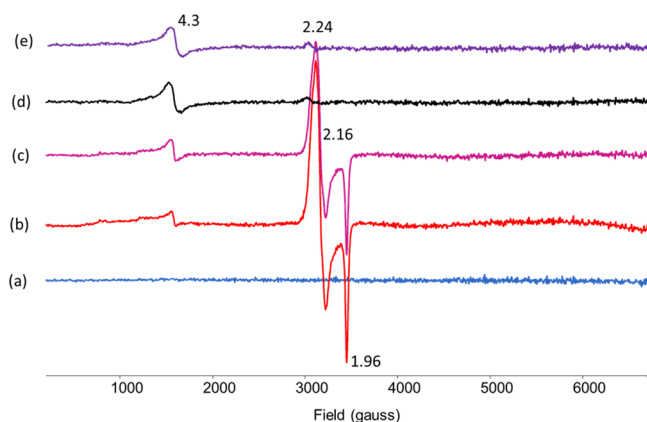


**Figure 11.** X band EPR spectra at 77 K of **1** in acetonitrile (1 mM) (a) before and (b) 15 s, (c) 40 s, (d) 120 s, and (e) 240 s after addition of 100 equiv of  $\text{H}_2\text{O}_2$ .

$\text{Fe}^{\text{III}}(\text{X})(\text{OOH})]^{2+}$  species (where X = solvent), which are close to those of bleomycin  $\text{Fe}^{\text{III}}\text{-OOH}$  ( $g = 1.95$ , 2.17, and 2.26).<sup>35</sup> Over time (60 s at 293 K) the signals at  $g = 2.24$ , 2.16, and 1.96, together with a weaker signal at ca.  $g = 4$  (vide infra), disappeared, with only a weak signal  $g = 4.3$  remaining. When water (1.25 M) was added prior to addition of 100 equiv of  $\text{H}_2\text{O}_2$ , only the weak signal at  $g = 4.3$  was observed at any time.

Addition of 10 equiv of  $\text{H}_2\text{O}_2$  to **1** in  $\text{CD}_3\text{CN}$  with  $\text{H}_2\text{O}$  (1 M) results in a shift of signals in the  $^1\text{H}$  NMR spectrum upfield, which is consistent with the formation of an antiferromagnetically coupled dimer (Figure S16), by comparison with the spectra of analogous dimers.<sup>11a,18,19a,36</sup>

**UV/Vis Absorption Spectroelectrochemistry.** The electrochemical oxidation and subsequent reduction of **1** under thin-layer conditions enable simultaneous recording of UV/vis absorption spectroscopy during cyclic voltammetry and the trapping of oxidation products at the electrode (Figure 12). **1** undergoes oxidation at 1.14 V in acetonitrile (vide supra), which is manifested in a decrease in the absorption bands at 359 and 429 nm and a minor increase in absorption at 310 nm (Figure 12). The changes were largely reversed upon reduction at ca. 1.1 V, although a full recovery of the initial spectrum was observed only at 0.2 V, which together with the absence of isosbestic points and the difference in  $I_{\text{p,a}}$  and  $I_{\text{p,c}}$  indicates partial chemical irreversibility, i.e., partial ligand exchange with adventitious water present in the electrolyte.

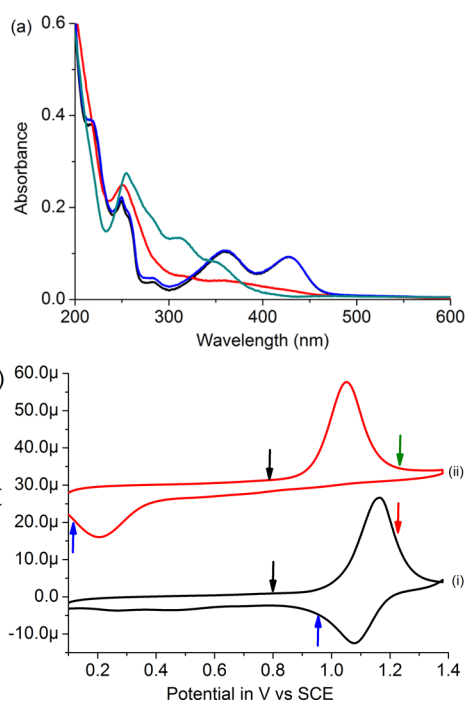


**Figure 12.** (a) UV/vis absorption spectra of **1** (1 mM) in acetonitrile before (black) and after electrochemical oxidation at  $>1.2$  V (red) and after subsequent reduction at 1.10 V (blue). The spectrum obtained with **1** (1 mM) in acetonitrile with water (0.36 M) at  $>1.2$  V is shown in green; the initial spectrum and spectrum recorded at 0.1 V (blue) were equivalent to the black and blue spectra, respectively. (b) Corresponding thin-layer cyclic voltammograms {(i) in  $\text{CH}_3\text{CN}$  and (ii) in  $\text{CH}_3\text{CN}$  with 0.36 M  $\text{H}_2\text{O}$  (offset by  $30 \mu\text{A}$  for clarity)}, with points at which spectra were recorded indicated by arrows, 0.1 M  $\text{TBAPF}_6$ , at 100  $\text{mV s}^{-1}$ .

Addition of water (0.36 M) to **1** (1 mM) in acetonitrile resulted in a minor decrease in visible absorbance (vide supra). Oxidation at 1.17 V was, in this case, completely irreversible, with a complete loss of absorbance at 429 nm and a concomitant increase in absorbance at 310 nm. Notably, reduction and recovery of the original spectrum were observed at  $<0.26$  V only under thin-layer conditions (Figure 12); however, a clear isosbestic point was maintained at 343 nm once reduction commenced. These data indicate that the irreversibility is due to exchange of solvent (i.e.,  $\text{H}_2\text{O}$  vs  $\text{CH}_3\text{CN}$  ligands) in the iron(III) oxidation state and confirm that this exchange is rapid.<sup>37</sup> Furthermore, it is apparent that although the presence of water has relatively little effect on **1** in the iron(II) state, in the iron(III) state its presence results in rapid ligand exchange and the formation of a stable dinuclear  $\text{Fe}^{\text{III}}\text{-(}\mu\text{-O)-Fe}^{\text{III}}$  complex, which is reduced only at 0.2 V.

In summary, it is evident that in the absence of water a mixture of  $[(\text{MeN3Py})\text{Fe}^{\text{III}}(\text{CH}_3\text{CN})_2]^{3+}$ ,  $[(\text{MeN3Py})\text{-Fe}^{\text{III}}(\text{CH}_3\text{CN})(\text{OH})]^{2+}$ , and  $[(\text{MeN3Py})\text{Fe}^{\text{III}}(\text{OH})_2]^+$  is formed upon oxidation of **1** in acetonitrile, which shows absorbance in the visible region. In the presence of water, rapid formation of an  $\text{Fe}^{\text{III}}\text{-(}\mu\text{-O)-Fe}^{\text{III}}$  species occurs with characteristic absorption bands<sup>38</sup> at 310 and 360 nm and reduction at ca. 0.2 V vs SCE.

**Effect of Acetic Acid on the Formation and Decay of  $[(\text{MeN3Py})\text{Fe}^{\text{III}}(\text{X})(\text{OOH})]^{2+}$ .** Addition of acetic acid (0.1 M) to **1** in acetonitrile does not affect its absorption spectrum or the extent of formation of the  $\text{Fe}^{\text{III}}\text{-OOH}$  species upon addition of

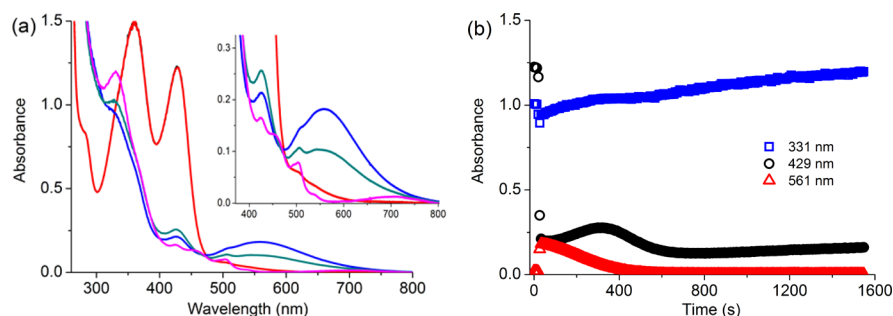


**Figure 13.** (a) UV/vis absorption of **1** (0.25 mM) in acetonitrile (black) and with acetic acid (100 equiv, red), immediately after addition of 100 equiv of  $\text{H}_2\text{O}_2$  (blue), after 200 s (green), and after 1527 s (pink). (b) Time dependence of the absorbance at 331 (blue), 429 (black), and 561 nm (red).

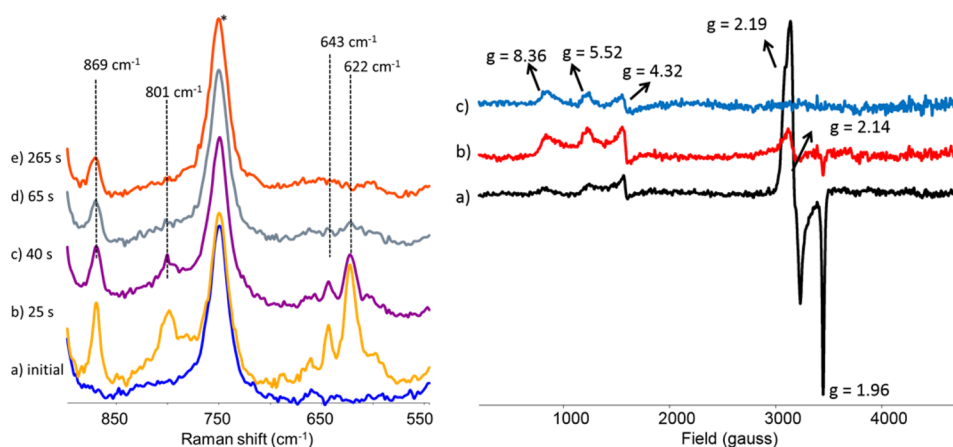


**Figure 14.** (Left) Resonance Raman spectra at  $\lambda_{\text{exc}}$  532 nm (a) before and (b) 25 s, (c) 40 s, (d) 65 s, and (e) 265 s after addition of 100 equiv of  $\text{H}_2\text{O}_2$  and (right) X-band EPR spectra (at 77 K) of flash frozen samples obtained (a) 20, (b) 44, and (c) 202 s after addition of 100 equiv of  $\text{H}_2\text{O}_2$  to **1** (1 mM) in acetonitrile with 0.1 M acetic acid. \*Raman spectra are normalized to the solvent band at  $750\text{ cm}^{-1}$ .

100 equiv of  $\text{H}_2\text{O}_2$  (Figure 13a). However, acetic acid affects the rate of formation and subsequent disappearance of the  $\text{Fe}^{\text{III}}\text{-OOH}$  species. Full conversion of **1** occurred within several seconds of addition of  $\text{H}_2\text{O}_2$  with an increase in absorbance at 551 nm (i.e.,  $\text{Fe}^{\text{III}}\text{-OOH}$ ) (Figure 13b). This absorption band decreased subsequently and more rapidly than without acetic acid and concomitant with an increase in absorbance at 310 nm. Notably, additional absorption bands that are characteristic of a  $[\{\text{LFe}^{\text{III}}\}_2(\mu\text{-O})(\mu\text{-CH}_3\text{CO}_2)]^{3+}$  complex were observed between 400 and 550 nm.<sup>34,39</sup> The formation of the latter species is apparent even prior to reaching a maximum in absorbance at 551 nm. Furthermore, closer inspection of the time dependence of the absorbance at 429 nm shows the appearance and disappearance of an additional intermediate also, assigned tentatively as  $[(\text{MeN}_3\text{Py})\text{Fe}^{\text{III}}(\text{OH})(\text{OH}_2)]^{2+}$ .

The presence of acetic acid (0.1 M) has no effect on the resonance Raman spectrum at  $\lambda_{\text{exc}}$  532 nm of the  $\text{Fe}^{\text{III}}\text{-OOH}$  species formed immediately upon reaction of **1** with  $\text{H}_2\text{O}_2$ ; that is, the resonantly enhanced bands are observed at 801, 643, and  $622\text{ cm}^{-1}$  (Figure 14, left). In contrast to that observed in the absence of acetic acid, however, the Raman band at  $869\text{ cm}^{-1}$  ( $\nu_{\text{O-O}}$  of  $\text{H}_2\text{O}_2$ ) persists for a considerable time after the disappearance of the bands at 801, 643, and  $622\text{ cm}^{-1}$ . Similarly, X-band EPR spectroscopy shows the appearance and disappearance of signals characteristic of a low-spin  $\text{Fe}^{\text{III}}\text{-OOH}$  species ( $g = 2.19, 2.14, 1.96$ ) concomitant with the absorption band at 551 nm. In addition a weaker signal ( $g = 8.36, 5.52,$

$4.32$ ) characteristic of a high-spin iron(III) complex is present and persists over the entire period with a maximum in intensity reached concomitant with the disappearance of the 551 nm absorption. It should be noted that, although much weaker, these signals are also discernible in the EPR spectra obtained without acetic acid (Figure 11). The appearance and disappearance of this latter EPR signal tracks the increase and decrease in absorbance at ca. 429 nm.

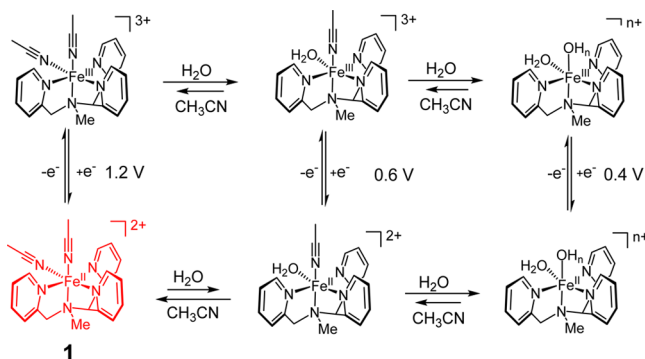
## DISCUSSION

The role of ligand exchange on the rate of formation of  $\text{Fe}^{\text{III}}\text{-OOH}$  species was studied through a combination of UV/vis absorption, resonance Raman,  $^1\text{H}$  NMR, and EPR spectroscopy, and electrochemistry. It is evident that although the formation of  $\text{Fe}^{\text{III}}\text{-OOH}$  species requires the presence of water to enable oxidation of **1** to its iron(III) state, the stability of these species and the rate of formation of  $\text{Fe}^{\text{III}}\text{-O-Fe}^{\text{III}}$  dimers (a thermodynamic sink) are also dependent on the concentration of water. The sensitivity of the system to even minor changes in water content is perhaps to be expected considering the highly nonlinear dependence of the activity of water on concentration.<sup>40</sup>

In acetonitrile, **1** shows two absorption bands in the visible region assigned to  $^1\text{MLCT}$  transitions. Addition of excess water results in a decrease in absorbance and a hypsochromic shift in the visible absorption bands, ultimately leading to a spectrum that is similar to that observed in water. In contrast to N5-ligand-based complexes such as  $[(\text{N}4\text{Py})\text{Fe}^{\text{II}}(\text{CH}_3\text{CN})]^{2+}$ , for

which addition of even 1 vol % acetonitrile to an aqueous solution results in a full recovery of the absorption spectrum seen in acetonitrile, in the case of **1** in water addition of up to 25 vol % has little effect on the spectrum.<sup>21</sup> This difference indicates that the barrier to exchange of both of the CH<sub>3</sub>CN ligands of **1** to form [(MeN3Py)Fe<sup>II</sup>(OH<sub>2</sub>)(CH<sub>3</sub>CN)]<sup>2+</sup> and [(MeN3Py)Fe<sup>II</sup>(OH<sub>2</sub>)<sub>2</sub>]<sup>2+</sup> is low compared with the corresponding N5-ligand-based complexes (Scheme 2). The

**Scheme 2. Redox-State-Dependent Ligand Exchange of CH<sub>3</sub>CN Ligands of **1** with Water<sup>a</sup>**



<sup>a</sup>It should be noted that the assignment of the ligands as aqua or hydroxido is arbitrary and is not confirmed in the present case.

exchange of the CH<sub>3</sub>CN ligands for H<sub>2</sub>O in **1** results in a decrease in oxidation potential and allows for ligand exchange with H<sub>2</sub>O<sub>2</sub>, both of which facilitate the initial oxidation from the iron(II) to the iron(III) state (vide infra).

Upon electrochemical oxidation of **1** to the iron(III) state, exchange of the CH<sub>3</sub>CN ligands with water becomes energetically highly favorable. Importantly, however, in the presence of excess water, oxidation and ligand exchange are followed rapidly by the formation of oxido-bridged dimers, which are reduced to the iron(II) state only at low potentials. Indeed the effect of water in facilitating the formation of oxido-bridged iron(III) dimers is manifested clearly in the differences observed by spectroelectrochemistry in the absence and presence of water. The effect of water on the spectroelectrochemical behavior is essentially the same as observed upon chemical oxidation with H<sub>2</sub>O<sub>2</sub>.

Addition of 1 equiv of H<sub>2</sub>O<sub>2</sub> to **1** in CH<sub>3</sub>CN results in only ca. 10% conversion to the iron(III) oxidation state. In contrast, with >0.1 M water, almost complete conversion of **1** to an EPR-silent complex is observed. Although with ca. 0.1 M H<sub>2</sub>O only partial (i.e., <10–15%) conversion of **1** to [(MeN3Py)Fe<sup>II</sup>(OH<sub>2</sub>)(CH<sub>3</sub>CN)]<sup>2+</sup> is observed, <sup>1</sup>H NMR spectroscopy and cyclic voltammetry confirm that the rate of exchange of the CH<sub>3</sub>CN ligands with water is high. Hence it is reasonable to conclude that formation of [(MeN3Py)Fe<sup>II</sup>(CH<sub>3</sub>CN)(OOH)]<sup>+</sup> or [(MeN3Py)Fe<sup>II</sup>(OH<sub>2</sub>)(OOH)]<sup>+</sup> can occur also followed by rapid heterolytic cleavage of the iron(II)-peroxy O–O bond<sup>33</sup> to form [(MeN3Py)Fe<sup>IV</sup>(OH<sub>2</sub>)(O)]<sup>2+</sup> and subsequent reaction with [(MeN3Py)Fe<sup>II</sup>(OH<sub>2</sub>)(CH<sub>3</sub>CN)]<sup>2+</sup> to form 2 equiv of [(MeN3Py)Fe<sup>III</sup>(OH<sub>2</sub>)(OH)]<sup>2+</sup>. The latter complex either undergoes further reaction with H<sub>2</sub>O<sub>2</sub> or undergoes dimerization to form EPR-silent (at 77 K) complexes, e.g., [(MeN3Py)Fe<sup>III</sup>(OH<sub>2</sub>)<sub>2</sub>(O)]<sup>4+</sup> (Scheme 3). Notably, however, in the absence of water, the Fe(III) complexes formed react more rapidly with H<sub>2</sub>O<sub>2</sub> (to decompose it) than does **1**. This difference in reactivity, together with the instability of both

the iron(II) and iron(III) peroxy species and Fe(IV) oxido species formed, results in only the initial complex **1** and the final Fe<sup>III</sup>–O–Fe<sup>III</sup> dimer being observed at significant concentrations.

It should be noted that addition of excess H<sub>2</sub>O<sub>2</sub> (25–100 equiv) results in the simultaneous addition of a similar excess of H<sub>2</sub>O (45–180 equiv). In this case the oxidation of **1** to the iron(III) state is rapid, aided by ligand exchange (CH<sub>3</sub>CN with H<sub>2</sub>O) in **1**, and is accompanied by the appearance of a visible absorption band that is characteristic of an Fe<sup>III</sup>–OOH species, which was confirmed by both resonance Raman and EPR spectroscopy. The decay of Fe<sup>III</sup>–OOH species formed is accelerated by the presence of water, and with >0.1 M H<sub>2</sub>O, the steady-state concentration of the Fe<sup>III</sup>–OOH species is too low to be observed despite both the rapid oxidation of **1** and the consumption of the excess H<sub>2</sub>O<sub>2</sub>. Indeed the UV/vis absorption and <sup>1</sup>H NMR spectra after oxidation (either electrochemical or with H<sub>2</sub>O<sub>2</sub>) together with the absence of a significant EPR signal indicate that essentially complete conversion to an Fe<sup>III</sup>–O–Fe<sup>III</sup> dimer occurs. ESI-MS data (see the Supporting Information) indicate the formation of various dinuclear Fe<sup>III</sup> complexes, although a definitive correlation between MS data and data obtained by other techniques is hampered by the conditions of the ESI-MS measurements. Notably the addition of acetic acid,<sup>41</sup> although not reacting directly with **1**, allows for full oxidation to the iron(III) state with fewer equivalents of H<sub>2</sub>O<sub>2</sub>, by suppressing the decomposition of H<sub>2</sub>O<sub>2</sub>. Furthermore, although acetato-bridged Fe<sup>III</sup>–O–Fe<sup>III</sup> dimers form in the presence of acetic acid,<sup>19</sup> there is no evidence that an acetate-bound Fe<sup>III</sup>–OOH species is formed. The effect of acetic acid in enhancing the efficiency of nonheme iron complexes in the oxidation of organic substrates has been noted frequently in earlier studies.<sup>19</sup> In the present study the suppression of H<sub>2</sub>O<sub>2</sub> decomposition by addition of acetic acid observed raises the possibility that in related systems this effect contributes substantially to the enhancement in the catalytic efficiency observed.

## CONCLUSIONS

In conclusion, the electrochemical and spectroscopic analysis demonstrates that the two CH<sub>3</sub>CN ligands of **1** undergo rapid ligand exchange with water, albeit with the equilibrium lying on the side of coordination of the CH<sub>3</sub>CN ligands. Nevertheless the decrease in redox potential when CH<sub>3</sub>CN is exchanged for water (or H<sub>2</sub>O<sub>2</sub>) allows for rapid oxidation of **1** to the iron(III) state presumably via an Fe<sup>IV</sup>=O intermediate generated by heterolysis of the O–O bond in an Fe<sup>II</sup>–OOH species. The exchange of water with CH<sub>3</sub>CN is the rate-determining step in the reaction of **1** with H<sub>2</sub>O<sub>2</sub> in CH<sub>3</sub>CN and competes with the decomposition of H<sub>2</sub>O<sub>2</sub> by the iron(III) complexes formed.

The formation of detectable amounts of an Fe<sup>III</sup>–OOH complex of an N4 ligand at room temperature depends critically on the concentration of water. As mentioned above the first role played by water is to accelerate the exchange of CH<sub>3</sub>CN ligands with H<sub>2</sub>O<sub>2</sub>. If this process is too slow, then the competing decomposition of H<sub>2</sub>O<sub>2</sub> will preclude reaching a significant steady-state concentration of the Fe<sup>III</sup>–OOH species. Hence water is needed to form the Fe<sup>III</sup>–OOH species. However, a second effect of water is to accelerate the formation of Fe<sup>III</sup>–O–Fe<sup>III</sup> dimers, which act as thermodynamic sinks preventing a buildup of a significant concentration of the Fe<sup>III</sup>–OOH species. This balance between assisting and inhibiting the formation of an Fe<sup>III</sup>–OOH species is of



wire auxiliary electrode, and an SCE reference electrode were employed. Unless stated otherwise all potential values are quoted with respect to the SCE. Potentials are reported  $\pm 10$  mV. Spectroelectrochemistry experiments were carried out by an OTTLE cell<sup>43</sup> (a liquid IR cell modified with Infrasil windows and a platinum mesh working and counter electrode and a Ag wire reference electrode) mounted in a Specord600 UV/vis spectrometer with potential controlled by a CHI600C potentiostat. Raman spectra were recorded at  $\lambda_{\text{exc}}$  785 nm using a PerkinElmer Raman Station at room temperature. Raman spectra at 457 nm (50 mW at source, Cobolt Lasers) and at 532 nm (300 mW at source, Cobolt Lasers) were obtained in a 135° and a 180° backscattering arrangement, respectively. Raman scattering was collected with a 2.5 cm diameter plano convex lens ( $f = 7.5$  cm). The collimated Raman scattering passed through an appropriate long pass edge filter (Semrock) and was focused by a second 2.5 cm diameter plano convex lens ( $f = 10$  cm) into a Shamrock300i spectrograph (Andor Technology) with a 1200 L/mm grating blazed at 500 nm and acquired with a Newton DU970N-BV or a iDus-420-BUE2 CCD camera (Andor Technology). The slit width was set to 80  $\mu\text{m}$ . Raman spectra at 355 nm (10 mW at source, Cobolt Lasers) were acquired in a 180° backscattering arrangement. Raman scattering was collected by a 2.5 cm diameter plano convex lens ( $f = 7.5$  cm). The collimated Raman scattering passed through an appropriate long pass edge filter (Semrock) and was focused by a second 2.5 cm diameter plano convex lens ( $f = 15$  cm) into a Shamrock500i spectrograph (Andor Technology) 2399 L/mm grating blazed at 300 nm, respectively, acquired with an iDus-420-BU2 CCD camera (Andor Technology). The spectral slit width was set to 12  $\mu\text{m}$ . Data were recorded and processed using Solis (Andor Technology) with spectral calibration performed using the Raman spectrum of acetonitrile/toluene, 50:50 (v/v).<sup>44</sup> Samples were held in quartz 10 mm path length cuvettes. Multipoint baseline correction was performed for all spectra. ESI-MS spectra recorded on a Triple Quadrupole LC/MS/MS mass spectrometer (API 3000, Perkin-Elmer Sciex Instruments). EPR spectra (X-band, 9.46 GHz) were recorded on a Bruker ECS106 spectrometer in liquid nitrogen (77 K). Samples for measurement that were followed from UV/vis absorption and an aliquot of 300  $\mu\text{L}$  were transferred to EPR tubes and were frozen in liquid nitrogen immediately.

## ■ ASSOCIATED CONTENT

### ■ Supporting Information

The Supporting Information is available free of charge on the ACS Publications website at DOI: [10.1021/acs.inorgchem.5b02976](https://doi.org/10.1021/acs.inorgchem.5b02976).

Additional Raman, UV/vis absorption, spectroelectrochemical, and <sup>1</sup>H NMR data (PDF)

## ■ AUTHOR INFORMATION

### ■ Corresponding Author

\*E-mail: [w.r.browne@rug.nl](mailto:w.r.browne@rug.nl). Tel: +31-503634428.

### ■ Notes

The authors declare no competing financial interest.

## ■ ACKNOWLEDGMENTS

Financial support comes from the European Research Council (ERC-2011-StG-279549, WRB), The Netherlands Fund for Technology and Science STW (11059, WRB), the Ministry of Education, Culture and Science (Gravity program 024.001.035, AD, WRB), and the Ubbo Emmius Fund of the University of Groningen (AD). The COST action CM1305 “Explicit control over spin-states in technology and biochemistry” is acknowledged for discussion.

## ■ REFERENCES

- (1) Abu-Omar, M. M.; Loaiza, A.; Hontzeas, N. *Chem. Rev.* **2005**, *105*, 2227–2252.
- (2) Costas, M.; Mehn, M. P.; Jensen, M. P.; Que, L., Jr. *Chem. Rev.* **2004**, *104*, 939–986.
- (3) Solomon, E. I.; Brunold, T. C.; Davis, M. I.; Kemsley, J. N.; Lee, S.-K.; Lehnert, N.; Neese, F.; Skulan, A. J.; Yang, Y.-S.; Zhou, J. *Chem. Rev.* **2000**, *100*, 235–350.
- (4) Girerd, J.-J.; Banse, F.; Simaan, A. J. *Struct. Bonding (Berlin)* **2000**, *97*, 143–177.
- (5) (a) Parales, R. E. *J. Ind. Microbiol. Biotechnol.* **2003**, *30*, 271–278. (b) Chakrabarty, S.; Austin, R. N.; Deng, D.; Groves, J. T.; Lipscomb, J. D. *J. Am. Chem. Soc.* **2007**, *129*, 3514–3515.
- (6) Que, L., Jr.; Tolman, W. B. *Nature* **2008**, *455*, 333–340.
- (7) Chen, K.; Costas, M.; Que, L., Jr. *J. Chem. Soc., Dalton Trans.* **2002**, 672–679. (b) Feng, J.; England, J.; Que, L., Jr. *ACS Catal.* **2011**, *1*, 1035–1042. (c) Suzuki, K.; Oldenburg, P. D.; Que, L., Jr. *Angew. Chem., Int. Ed.* **2008**, *47*, 1887–1889.
- (8) Ensley, B. D.; Gibson, D. T. *J. Bacteriol.* **1983**, *155*, 505–511.
- (9) Roelfes, G.; Vrajmisu, V.; Chen, K.; Vrajmisu, K.; Ho, R. Y. N.; Rohde, J.-U.; Zondervan, C.; la Crois, R. M.; Schudde, E. P.; Lutz, M.; Spek, A. L.; Hage, R.; Feringa, B. L.; Munck, E.; Que, L., Jr. *Inorg. Chem.* **2003**, *42*, 2639–2653.
- (10) Simaan, A. J.; Döpner, S.; Banse, F.; Bourcier, S.; Bouchoux, G.; Boussac, A.; Hildebrandt, P.; Girerd, J. J. *Eur. J. Inorg. Chem.* **2000**, *2000*, 1627–1633.
- (11) (a) Chen, K.; Que, L., Jr. *J. Am. Chem. Soc.* **2001**, *123*, 6327–6337. (b) Chen, K.; Costas, M.; Kim, J.; Tipton, A. K.; Que, L., Jr. *J. Am. Chem. Soc.* **2002**, *124*, 3026–3035. (c) Prat, I.; Mathieson, J. S.; Guell, M.; Ribas, X.; Luis, J. M.; Cronin, L.; Costas, M. *Nat. Chem.* **2011**, *3*, 788–793.
- (12) The presence of acetic acid is proposed by Wang et al. to change the catalytic pathway dramatically, precluding formation of such iron(V)=O species. Wang, Y.; Janardanan, D.; Usharani, D.; Han, K.; Que, L., Jr.; Shaik, S. *ACS Catal.* **2013**, *3*, 1334–1341.
- (13) (a) Chen, K.; Que, L., Jr. *Chem. Commun.* **1999**, 1375–1376. (b) Kim, C.; Chen, K.; Kim, J.; Que, L., Jr. *J. Am. Chem. Soc.* **1997**, *119*, 5964–5965. (c) Hirao, H.; Li, F.; Que, L., Jr.; Morokuma, K. *Inorg. Chem.* **2011**, *50*, 6637–6648.
- (14) Klopstra, M.; Roelfes, G.; Hage, R.; Kellogg, R. M.; Feringa, B. L. *Eur. J. Inorg. Chem.* **2004**, *2004*, 846–856.
- (15) (a) Burger, R. M.; Kent, T. A.; Horwitz, S. B.; Muenck, E.; Peisach, J. *J. Biol. Chem.* **1983**, *258*, 1559–1564. (b) Sam, J. W.; Tang, X.-J.; Peisach, J. *J. Am. Chem. Soc.* **1994**, *116*, 5250–5256. (c) Loeb, K. E.; Zaleski, J. M.; Westre, T. E.; Guajardo, R. J.; Mascharak, P. K.; Hedman, B.; Hodgson, K. O.; Solomon, E. I. *J. Am. Chem. Soc.* **1995**, *117*, 4545–4561.
- (16) Makhlynets, O. V.; Oloo, W. N.; Moroz, Y. S.; Belaya, I. G.; Palluccio, T. D.; Filatov, A. S.; Muller, P.; Cranswick, M. A.; Que, L., Jr.; Rybak-Akimova, E. V. *Chem. Commun.* **2014**, *50*, 645–648.
- (17) (a) Chen, K.; Costas, M.; Kim, J. H.; Tipton, A. K.; Que, L., Jr. *J. Am. Chem. Soc.* **2002**, *124*, 3026–3035. (b) Oloo, W. N.; Fielding, A. J.; Que, L., Jr. *J. Am. Chem. Soc.* **2013**, *135*, 6438–6441. (c) Mas-Balleste, R.; Que, L., Jr. *J. Am. Chem. Soc.* **2007**, *129*, 15964–15972.
- (18) Roelfes, G.; Lubben, M.; Chen, K.; Ho, R. Y. N.; Meetsma, A.; Genseberger, S.; Hermant, R. M.; Hage, R.; Mandal, S. K.; Young, V. G.; Zang, Y., Jr.; Kooijman, H.; Spek, A. L.; Que, L., Jr.; Feringa, B. L. *Inorg. Chem.* **1999**, *38*, 1929–1936.
- (19) (a) White, M. C.; Doyle, A. G.; Jacobsen, E. N. *J. Am. Chem. Soc.* **2001**, *123*, 7194–7195. (b) Chen, M. S.; White, M. C. *Science* **2007**, *318*, 783–787. (c) Chen, M. S.; White, M. C. *Science* **2010**, *327*, 566–571. (d) White, M. C. *Science* **2012**, *335*, 807–809.
- (20) Zang, Y.; Kim, J.; Dong, Y.; Wilkinson, E. C.; Appelman, E. H.; Que, L., Jr. *J. Am. Chem. Soc.* **1997**, *119*, 4197–4205.
- (21) Draksharapu, A.; Li, Q.; Logtenberg, H.; van den Berg, T. A.; Meetsma, A.; Killeen, J. S.; Feringa, B. L.; Hage, R.; Roelfes, G.; Browne, W. R. *Inorg. Chem.* **2012**, *51*, 900–913.
- (22) Puri, M.; Que, L., Jr. *Acc. Chem. Res.* **2015**, *48*, 2443–2452.

(23) The shift to less positive potentials is due to electrostatic stabilization of the Fe(III) state by water.

(24) Streckas, T. C.; Mandal, S. K. *J. Raman Spectrosc.* **1984**, *15*, 109–112.

(25) Although the maximum of this band is at 551 nm, for analysis of the time dependence of the appearance and disappearance of this band independent of absorbance of **1**, 561 nm was selected as monitoring wavelength.

(26) These data indicate that the molar absorptivity is greater than  $560 \text{ M}^{-1} \text{ cm}^{-1}$ .

(27) It should be noted in the case of cyclohexene that the alkylperoxides present cause immediate oxidation of **1** to the Fe(III) state. Nevertheless subsequent addition of  $\text{H}_2\text{O}_2$  leads to the formation of the same Fe(III)–OOH species as observed without cyclohexene. These reactive impurities are removed by passing the alkene over alumina immediately prior to use, and in this case the same results were obtained as with cyclooctene.

(28) A higher concentration (1 mM) was used for resonance Raman studies at 532 nm and EPR spectroscopy to increase S/N levels. UV/vis absorption spectra under these conditions show essentially the same changes as **1** at 0.25 mM.

(29) The availability of  $^{18}\text{O}$ -labeled  $\text{H}_2\text{O}_2$  only as dilute solutions in water precludes assignment of the Raman bands of the Fe<sup>III</sup>–OOH species by isotopic labeling.

(30) Ho, R. Y. N.; Roelfes, G.; Hermant, R.; Hage, R.; Feringa, B. L.; Que, L., Jr. *J. Am. Chem. Soc.* **1999**, *121*, 264–265.

(31) McGarvey, J. J.; Draksharapu, A.; Browne, W. R. *Special Periodic Reports* **2013**, *44*, 68–94.

(32) Bukowski, M. R.; Comba, P.; Limberg, C.; Merz, M.; Que, L., Jr.; Wistuba, T. *Angew. Chem., Int. Ed.* **2004**, *43*, 1283–1283.

(33) Draksharapu, A.; Angelone, D.; Quesne, M. G.; Padamati, S. K.; Gomez, L.; Hage, R.; Costas, M.; Browne, W. R.; de Visser, S. P. *Angew. Chem., Int. Ed.* **2015**, *54*, 4357–4361.

(34) Payeras, A. M.; Ho, R. Y. N.; Fujita, M.; Que, L., Jr. *Chem. - Eur. J.* **2004**, *10*, 4944–4953.

(35) (a) Burger, R. M.; Peisach, J.; Honvitz, S. B. *J. Biol. Chem.* **1981**, *256*, 11636–11644. (b) Veselov, A.; Sun, H.; Sienkiewicz, A.; Taylor, H.; Burger, R. M.; Scholes, C. P. *J. Am. Chem. Soc.* **1995**, *117*, 7508–7512.

(36) Dong, Y.; Fujii, H.; Hendrich, M. P.; Leising, R. A.; Pan, G.; Randall, C. R.; Wilkinson, E. C.; Zang, Y.; Que, L., Jr.; Fox, B. G.; Kauffmann, K.; Munck, E. *J. Am. Chem. Soc.* **1995**, *117*, 2778–2792.

(37) The spectroelectrochemical studies were carried out under thin-layer conditions in which the diffusion of products away from the electrode is prevented and a relatively high concentration of **1** and low concentration of water are used (comparable with Figure 4b). The entire sample undergoes oxidation to the Fe<sup>III</sup> state and ligand exchange with water, providing a high concentration from which an Fe<sup>III</sup>–O–Fe<sup>III</sup> species forms quantitatively. Due to the thin-layer conditions  $E_{p,c}$  is shifted positively compared with solution-based voltammetry, and although two reduction waves would be expected, a single wave is observed, as the initial reduction to the Fe(II)–O–Fe(III) species results in formation of **1** and LFe(III)–OH, with the latter species undergoing reduction and immediate conversion to **1**, as the overpotential is already several –100 mV for its reduction. The Nernst equilibrium between Fe(III)–O–Fe(III) and Fe(II)–O–Fe(III) will be reestablished concomitantly, and hence only the first reduction wave is observed.

(38) Zart, M. K.; Powell, D.; Borovik, A. S. *Inorg. Chim. Acta* **2007**, *360*, 2397–2402.

(39) Norman, R. E.; Yan, S.; Que, L., Jr.; Sanders-Loehr, J.; Backes, G.; Ling, J.; Zhang, J. H.; O'Connor, C. J. *J. Am. Chem. Soc.* **1990**, *112*, 1554–1562.

(40) A long-standing difficulty in the use of concentration as a proxy for activity in water/acetonitrile is the highly nonlinear dependence of the activity of water on its concentration. Indeed the activity of water rises sharply as its mole fraction is increased from 0 to 0.2 to near unit activity. French, H. T. *J. Chem. Thermodyn.* **1987**, *19*, 1155–1161. For

a detailed discussion of this issue see: Blandamer, M. J.; Engberts, J. B. F. N.; Gleeson, P. T.; Reis, J. C. R. *Chem. Soc. Rev.* **2005**, *34*, 440–458.

(41) Oloo, W. N.; Meier, K. K.; Wang, Y.; Shaik, S.; Munck, E.; Que, L., Jr. *Nat. Commun.* **2014**, *5*, 3046–3054.

(42) The source of  $\text{H}_2\text{O}_2$  used can in some circumstances have a large effect on the results obtained due to the stabilizers present: 50%  $\text{H}_2\text{O}_2$  supplied by Sigma-Aldrich “Contains proprietary inorganic tin-based stabilizer”, whereas the 50%  $\text{H}_2\text{O}_2$  PA grade and 30% medicinal grade supplied by Acros are stabilized by organic chelating agents and by  $\text{Na}_2\text{H}_2\text{P}_2\text{O}_7$ ,  $\text{H}_3\text{PO}_4$ , and  $\text{NH}_4\text{NO}_3$ , respectively. In the present study the source of  $\text{H}_2\text{O}_2$  used had no noticeable effect on the data obtained, which may be due to the limited number of equivalents of  $\text{H}_2\text{O}_2$  used with respect to **1**, and hence the concentration of stabilizer present is low compared with the catalyst.

(43) Krejčík, M.; Daněk, M.; Hartl, F. *J. Electroanal. Chem. Interfacial Electrochem.* **1991**, *317*, 179–186.

(44) McCreery, R. L. *Raman Spectroscopy for Chemical Analysis*; John Wiley & Sons: New York, USA, 2000; pp 259–260.